Distributed Co-Phasing with Autonomous Constellation Selection

Ribhu Chopra, Ramesh Annavajjala, and Chandra R. Murthy

***Abstract*—In this paper, we consider a distributed co-phasing (DCP) technique where multiple sensor nodes (SNs) communicating their observations to a fusion center (FC) need to transmit different classes of data requiring different levels of error protection. To achieve this, we propose a variant of the DCP technique with autonomous constellation selection at the different SNs. In the first stage of this two stage time division duplexed (TDD) co-phasing scheme, the SNs obtain estimates of the channels to the FC using pilot symbols transmitted by the latter. Following this, the SNs simultaneously transmit their data symbols pre-rotated according to the estimated channel phases to combine coherently at the FC. The symbols transmitted by different SNs are drawn from different constellations selected based on the estimated instantaneous channel gains. We show that this scheme is equivalent to transmitting symbols from hierarchical constellations. Based on the properties of hierarchical constellations, we develop recursive expressions for the BER of the proposed system. Following this, we use the properties of the effective channel coefficients to show that it is possible to recover the transmitted data bits from the signal received at the FC blindly, without requiring explicit pilot symbols to be sent by the power starved SNs. We develop three blind channel estimation and data detection schemes for the presented system model. Using Monte Carlo simulations, we show that the proposed blind channel estimation algorithm achieves a probability of error performance close to that with genie aided perfect CSI at the FC, while using only a moderate number of unknown data symbols for channel estimation.**

***Index Terms*—Distributed co-phasing, wireless sensor networks, data fusion, hierarchical constellations, adaptive Modulation, blind channel estimation**

I. Introduction

Wireless sensor networks (WSNs) are seen as a major enabling technology for the internet of things (IoT) [1], [2]. A WSN consists of a set of low power sensor nodes (SNs) observing a physical phenomenon and communicating their observations to a fusion center (FC) [3]. The communication of data from the SNs to the FC, known as data fusion, is a challenging problem due to constraints on the processing capabilities of SNs [3], [4] and diverse requirements on the reliability of the parameters measured by the SNs. Distributed co-phasing (DCP), based on the idea of distributed transmit beamforming (DTB), is a class of physical layer techniques that can be used for data fusion in WSNs [5]. The underlying idea behind DCP is to use the transmitting nodes as a distributed antenna array to achieve coherent combining gain as well as diversity gain at the FC. DCP systems employ fixed power transmission from the nodes, and can therefore function with low-cost power amplifiers. The feasibility of DCP in practical implementations is well established, and so is its robustness to channel estimation errors [6], [7]. Moreover, when the signals coherently combine at the intended receiver, they naturally combine incoherently at any unintended location, thereby making DCP inherently secure.

DCP is a two stage communication technique. During the first stage, known pilot symbols are transmitted by the FC to the SNs. These pilots are used by the SNs to estimate their respective channels to the FC. The training of the SNs by the FC is desirable due to multiple reasons. Firstly, it shifts the load of the power intensive training operation from the battery powered SNs to the FC which is generally connected to the mains. Secondly, this significantly reduces the training overhead in comparison to forward link training, that involves each of the SNs training the FC in orthogonal training durations. In the second stage, the SNs pre-rotate their data to compensate for the estimated channel phase and then synchronously transmit. Such a transmission scheme works when the channel is quasi static and reciprocal [6], [8]. The pre-rotation of data by the SNs ensures coherent combining of different transmitted signals at the FC, resulting in coherent combining gains and diversity gains. However, in its current form, DCP provides fixed levels of error protection to different bit streams [9]; whereas it may be desired to provide different classes of bits flexible levels of error protection. For example, it may be necessary to provide the bits corresponding to alarms and interrupts with a higher order of protection in comparison to the bits corresponding to detailed system information. In this work, our main focus is to use the channel gain estimates at different SNs in conjunction with adaptive constellation selection (ACS) to achieve unequal error protection (UEP) for different classes of bits in a DCP system. Further, we are interested in analyzing the amount of service level differentiation that such an approach can offer, and its implication on the design of data fusion schemes in WSNs.

A. Related Work

The idea of UEP of two or more classes of data was first proposed in the pioneering work of Cover on broadcast channels [10]. In this scheme, the more basic or coarse data is provided a higher level of protection and is recoverable by a larger number of receivers than the less important or detailed data. It has since been shown that UEP can practically be

R. Chopra was with the Indian Institute of Science, Bangalore, India. He is now with the Indian Institute of Technology Guwahati, Assam, India. R. Annavajjala is affiliated with the Northeastern University, Boston, MA, USA. C. R. Murthy is with the Indian Institute of Science, Bangalore, India. Emails: ribhu@outlook.com, cmurthy1@gmail.com, ramesh.annavajjala@gmail.com.

The work of C. R. Murthy was financially supported by the Young Faculty Research Fellowship from the Ministry of Inform. Technology, Govt. of India.

achieved in conventional point to point communication systems by employing hierarchical modulation at the transmitter [11], [12]. This was studied for systems supporting different classes of traffic, each with a different quality of service (QoS) requirement [13], such as multimedia services [14], [15] and digital television broadcasting [11]. The recursive technique for BER calculation in QAM systems developed in [16] was extended in [17] for BER calculations in broadcast based hierarchical modulation systems. The performance improvement offered by hierarchical constellations over conventional non-hierarchical constellations with and without layered source encoding is examined in [18]. In [19], the authors generalize the conventional two layer UEP using hierarchical modulation to a J layer UEP.

In this work, our main aim is to provide unequal error protection to different classes of bits being communicated by the SNs via DTB. It was shown in [4] and [6] that it is possible for multiple SNs to transmit coherently to an FC. The feasibility of perfect carrier synchronization among different SNs was demonstrated in [6], [20]. The performance loss in DTB schemes due to imperfections in the channel estimates is quantified in [21]. The applicability of DTB for systems with multiple transmit and receive antennas has also been discussed in [9], [22]–[24].

The performance of various DTB schemes viz. DCP, maximal ratio transmission, censored transmission and truncated channel inversion for constant modulus constellations is compared in [7]. Following this, it is shown in [25] that the received data symbols can be used for blind channel estimation. This allows DCP based systems to use non constant modulus constellations, thus increasing the achievable spectral efficiency per channel use. The single antenna FC DCP framework has been extended to a multi-antenna FC in [9], where it is shown that the achievable spectral efficiency of a DCP system can be increased by transmitting multiple data streams to the FC. However, earlier works on DCP disregard the channel gain information available at the SNs and transmit all the data bits regardless of the channel quality. Additionally, the present works on DCP consider that the same constellation is used by all the transmitting SNs.

B. Contributions

In the present work, we consider the case where each SN selects its transmit constellation autonomously, based on its estimated channel gain. Following this, each SN transmits symbols from the selected constellation to the FC after co-phasing them to compensate for the channel phase. It is shown that this results in the received signal being drawn from a *hierarchical constellation* whose parameters are determined by the constellation selection scheme at the SNs. However, since neither the channel gains, nor the constellation preferences of different nodes are available at the FC, it becomes challenging to detect the received data symbols.

The main objective of this paper is to devise a DCP system providing unequal error protection to different classes of data using ACS at different SNs. Our contributions are as follows:

1) We show that using ACS in a DCP system is equivalent to using hierarchical constellations in a point to point system. (See Section II.)
2) We derive the statistics of the effective DCP channels for different bits as seen by the FC for a straight binary encoded DCP system with ACS. (See Section III.)
3) We develop recursive expressions for calculating the error rates for different bit streams under perfect CSI at the SNs and the FC. (See Section IV.)
4) We use the properties of the effective channel coefficients to devise three blind channel estimation algorithms for the proposed system. (See Section V.)
5) We use the BER analysis under perfect CSI to derive the performance of the system under estimated CSI at SNs and the FC. (See Section VI.)
6) Via detailed simulations, we validate the derived theory and compare the performance of the three proposed blind channel estimation algorithms. (See Section VII.)

Therefore, the proposed DCP-ACS scheme can be used to provide unequal error protection to different bits in a wireless sensor network. The blind channel estimation algorithms discussed in this work can be independently useful for decoding hierarchical constellations in point to point systems.

Notation: Boldface lowercase and uppercase letters represent vectors and matrices, respectively. The kth column of the matrix $\mathbf{A}$ is denoted by $\mathbf{a}_k$, and $\mathbf{a}^{(k)}$ represents its kth row. $(.)^H$ represents the hermitian operation on a vector or a matrix. $\|\cdot\|_2$ and $\|\cdot\|_F$ respectively represent the ℓ_2 norm of a vector and the Frobenius norm of a matrix. $E[\cdot]$ and $\text{var}(\cdot)$ represent the mean and variance of a random variable.

Next, we describe the system model considered in this work.

II. System Model

We consider a wireless sensor network consisting of K SNs communicating M classes of data to a single antenna FC. Each class of data requires a different level of protection against errors induced by fading and receiver noise. Since there are multiple classes of data, and each SN independently chooses the classes that it wants to transmit. As a consequence, the data being transmitted by the different SNs could be different. The system model is illustrated in Fig. 1.

In DCP, the SNs and the FC communicate over two time division duplexed stages. In the first stage, the FC broadcasts N_p pilots. These pilots are used by the K SNs to estimate the coefficients of the K channels between themselves and the FC. In the second stage, consisting of N_d channel uses, the SNs synchronously transmit their selected classes of data to the FC. It has been practically demonstrated in [5] that once synchronized, the SNs remain in synchronism for durations much longer than the channel coherence time, and therefore they can transmit synchronously. Here, we assume the channel to be block-fading, such that it remains constant throughout a frame consisting of training and data durations [5], [6] and varies independently from frame to frame. Also, the channels between the FC and the SNs are assumed exhibit reciprocity [7], which is a necessary condition for signals to combine coherently at the FC in DCP.

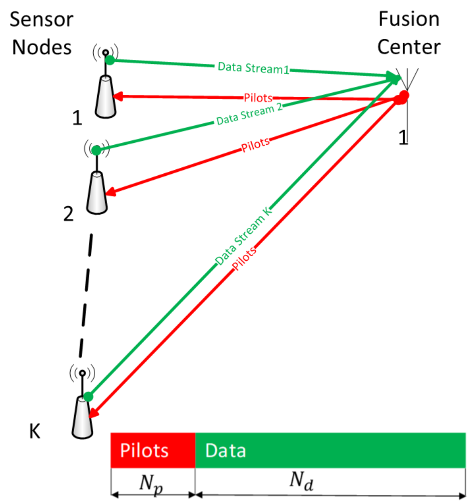

Figure 1. The DCP system model.

The training signal received by the kth SN during the nth channel use, $n \in \{1, \ldots, N_p\}$ can be written as

$$y_k[n] = \alpha_k e^{j\theta_k} \sqrt{\mathcal{E}_p} + w_k[n], \tag{1}$$

where $\mathcal{E}_P$ is the pilot power, α_k is the Rayleigh distributed channel gain with $E[|\alpha_k|^2] \triangleq \Omega_k$, θ_k is the uniformly distributed channel phase, and $w_l[n]$ is the zero mean circularly symmetric complex additive white Gaussian noise (AWGN) with per dimension variance $\frac{N_0}{2}$.

The maximum likelihood (ML) estimate of the channel phase at the kth SN is given as [7]

$$\hat{\theta}_k = \tan^{-1}\left(\frac{\sum_{n=1}^{N_p} \Im\{y_k[n]\}}{\sum_{n=1}^{N_p} \Re\{y_k[n]\}}\right), \tag{2}$$

where $\Re\{.\}$ and $\Im\{.\}$ represent the real and imaginary parts of a complex number, respectively. In conventional DCP, the nodes transmit common data using symbols from the same constellation, and ignore the channel gain information available from the training symbols. The use of channel gain estimates in addition to the phase estimates can potentially improve the performance of DCP. However, since WSN applications typically require the nodes to transmit at fixed power levels to simplify the RF power amplifier design, it is not possible to use power control.[1] Consequently, we propose to use the channel gain information for autonomous constellation selection at each node. The ML channel estimate at the kth node can be shown to take the form [7],

$$\hat{\alpha}_k = \sqrt{\frac{1}{\mathcal{E}_p}\left(\frac{1}{N_p}\sum_{n=1}^{N_p} |y_k[n]|^2 - N_0\right)}. \tag{3}$$

Each node then uses the estimated channel gain to decide on the symbol constellation to use for data transmission. If the estimated channel from a given node to the FC is poor, then the node transmits using a lower order constellation, thereby sending only the bits requiring the highest error protection. On the other hand, if the channel is good, symbols from a higher order constellation are transmitted, enabling the SN to communicate higher priority data bits in addition to the lower priority data bits. The key idea in ACS is that the SNs independently decide on the number of bits to transmit to the FC, based on their estimated channel gains. This makes the scheme considered in this paper different from previous work on DCP [7], [9], [25], where the SNs are assumed to transmit symbols from the same constellation regardless of the estimated channel gain.

Now, since the nodes need to communicate a total of M bits belonging to different classes, each node can perform constellation selection by binning the channel gain estimate to one of the M non-overlapping intervals, and mapping each of these intervals to a constellation choice. These M intervals can be expressed in terms of their boundaries $\tau_1, \tau_2, \ldots, \tau_M$, with the kth node transmitting symbols from a binary constellation denoted by $\mathcal{S}_1$ if $\hat{\alpha}_k \leq \tau_1$, from a quaternary constellation, $\mathcal{S}_2$, if $\tau_1 < \hat{\alpha}_k \leq \tau_2$, and similarly from a 2^m-ary constellation, denoted by $\mathcal{S}_m$, if $\tau_{m-1} < \hat{\alpha}_k \leq \tau_m$. Here, we define $\tau_0 = 0$ and $\tau_M = \infty$. Thus, based on the estimated channel to the FC, the kth node selects the symbol $s_k[n] \in \mathcal{S}_m$, and pre-rotates it to compensate for the estimated channel phase $\hat{\theta}_k$ such that the symbol transmitted by the kth node becomes $x_k[n] = \sqrt{\mathcal{E}_s} s_k[n] e^{-j\hat{\theta}_k}$.

In this work, we consider lattice based constellations for ACS at the nodes, and focus on 1 and 2 dimensional constellations. Specifically, we consider PAM based constellations for the 1-d ACS and QAM based constellations for the 2-d ACS. We describe the received signal models these for two cases in the following two subsections.

A. Received Signal Model for PAM Constellations

We first consider the case where each node transmits from one of M possible PAM constellations. For a straight binary encoded 2^m-PAM constellation, each symbol is a linear combination of a bipolar representation of the individual bits. That is, if the ith bit of the lth constellation symbol, s_l, for an m $(1 \leq m \leq M)$ bit PAM-constellation is represented by $b_{l,i}[n]$, with $b_{l,i}[n] \in \{-1, 1\}$, then s_l can be expressed as

$$s_l[n] = \sum_{m=1}^{M} g_m(\hat{\alpha}_k) b_{l,i}[n]. \tag{4}$$

In the above equation,

$$g_m(\hat{\alpha}_k) \triangleq \sum_{i=1}^{M} g_{mi} \mathbb{1}_{\{\tau_{i-1} \leq \hat{\alpha}_k < \tau_i\}}, \tag{5}$$

with g_{mi} being the weight assigned to the mth bit when $\hat{\alpha}_k$ lies in the ith interval, and $\mathbb{1}_{\{.\}}$ being the indicator function.

For example, consider a 2/4 PAM DCP-ACS where the kth SN transmits a BPSK signal when $\hat{\alpha}_k \leq \tau_1$ and a 4-PAM signal if $\hat{\alpha}_k > \tau_1$, using a symbol energy ($\mathcal{E}_s$) for transmission. Then, the symbol transmitted by it at the nth instant, $s_k[n]$,

[1]An analysis on the use of power control in DCP based systems can be found in [7].

can be written as

$$s_k[n] = \begin{cases} \sqrt{\mathcal{E}_s} b_1[n] e^{-j\hat{\theta}_k} & \hat{\alpha}_k \leq \tau_1 \\ b_1[n]\sqrt{\frac{4\mathcal{E}_s}{5}} e^{-j\hat{\theta}_k} + b_2[n]\sqrt{\frac{\mathcal{E}_s}{5}} e^{-j\hat{\theta}_k} & \hat{\alpha}_k > \tau_1. \end{cases} \tag{6}$$

which can be represented compactly using (4) and (5) with $g_{11} = 1$, $g_{21} = 0$, $g_{12} = \frac{2}{\sqrt{5}}$, and $g_{22} = \frac{1}{\sqrt{5}}$. Using these, we can now write the signal received at the fusion center at the nth time instant ($n \in [N_p + 1, N_p + N_d]$) as

$$y[n] = \sum_{k=1}^{K} (g_1(\hat{\alpha}_k) b_1[n] + g_2(\hat{\alpha}_k) b_2[n]) \sqrt{\mathcal{E}_s} \alpha_k e^{j(\theta_k - \hat{\theta}_k)} + w[n]. \tag{7}$$

Defining the effective channel for the mth bit as

$$h_m \triangleq \sum_{k=1}^{K} g_m(\hat{\alpha}_k) \alpha_k e^{j(\theta_k - \hat{\theta}_k)}, \tag{8}$$

we can rewrite $y[n]$ as

$$y[n] = h_1 \sqrt{\mathcal{E}_s} b_1[n] + h_2 \sqrt{\mathcal{E}_s} b_2[n] + w[n]. \tag{9}$$

This is the same as a 2/4 hierarchical constellation with h_1 and h_2 being the effective channel coefficients for the two bits, which are referred to as the *mean distance to the two bits* in the hierarchical modulation literature [26].

Now, since each symbol for a 2^M-ary straight binary encoded PAM can also be expressed as a linear combination of the bipolar representations of its individual bits, the 2/4 PAM model can be extended to a $2/4/\ldots/2^M$ PAM. In this case, $y[n]$ becomes $y[n] = \sum_{m=1}^{M} h_m \sqrt{\mathcal{E}_s} b_m[n] + w[n]$.

The effective channel vector for 2^M PAM can therefore be expressed as

$$\mathbf{h} = [h_1, \ldots, h_M]^T. \tag{10}$$

The BER for each individual bit is determined by the values of h_ms, which in turn depend on the thresholds $\tau_0, \ldots, \tau_M$. Therefore, the error protection offered to different bits can be controlled by suitably selecting these thresholds. For example, if $\tau_0 = 0, \tau_1 = \tau_2 = \cdots = \tau_M = \infty$, all nodes only transmit the MSB, $b_1[n]$, using BPSK, leading to the best possible error protection for $b_1[n]$; and the lower order bits are not transmitted at all. On the other hand, if $\tau_0 = \tau_1 = \cdots = \tau_{M-1} = 0$, all nodes transmit all bits regardless of channel state, and therefore, all bits are offered nearly equal error protection.

B. Received Signal Model for QAM Constellations

Let us first consider a system where each node transmits using either BPSK or QPSK based on the channel state, that is, the transmit signal $s_k[n]$ takes the form

$$s_k[n] = \begin{cases} \sqrt{\mathcal{E}_s} b_1[n] e^{-j\hat{\theta}_k} & \hat{\alpha}_k \leq \tau_1 \\ \sqrt{\frac{\mathcal{E}_s}{2}} b_1[n] e^{-j\hat{\theta}_k} + j\sqrt{\frac{\mathcal{E}_s}{2}} b_2[n] e^{-j\hat{\theta}_k} & \hat{\alpha}_k > \tau_1. \end{cases} \tag{11}$$

Writing h_m as the effective channel gain for the mth bit, the received signal at the FC takes the form

$$y[n] = h_1 \sqrt{\mathcal{E}_s} b_1[n] + j h_2 \sqrt{\mathcal{E}_s} b_2[n] + w[n] \tag{12}$$

where h_m is defined in (8), with $g_{11} = 1, g_{21} = 0$, and $g_{12} = g_{22} = \frac{1}{\sqrt{2}}$. Hence, sending BPSK and QPSK signals from different nodes based on their channel estimates corresponds to sending a hierarchical QPSK signal with the powers of the in-phase and quadrature components being controlled by the threshold τ_1.

Now, since any QAM constellation can be represented as a combination of two orthogonal PAMs, we can generalize the above received signal model to a $2M$ bit constellation, with the odd bits being sent over the in-phase component and the even bits being sent over the quadrature component, as follows:

$$y[n] = \sum_{m=1}^{M} h_{2m-1} \sqrt{\mathcal{E}_s} b_{2m-1}[n] + j h_{2m} \sqrt{\mathcal{E}_s} b_{2m}[n] + w[n]. \tag{13}$$

We can define the $2M$ dimensional effective channel similar to (10).

Now, in order to analyze the performance of the above hierarchical DCP system resulting from ACS at the individual SNs, we need to analyze the statistics of the effective channels. The past work on DCP considers a single constellation being employed at all nodes irrespective of the channel state. In contrast, in this work, since the number of bits being transmit by each node depends on the channel gains, the effective channel coefficients become different for different bits. Due to this, previous analysis of DCP based systems does not apply to our system. In the next section, we derive the statistics of the effective channel under both perfect and estimated CSI at the SNs. In Sec. IV, we use the derived channel statistics to analyze the BER performance.

III. Channel Statistics

A. Channel Statistics with Perfect CSI at the SNs

Consider the case where perfect CSI is available at each SN, so that $\hat{\alpha}_k = \alpha_k$ and $\hat{\theta}_k = \theta_k$. Substituting (5) into (8) we get

$$h_m = \sum_{k=1}^{K} \sum_{i=1}^{M} g_{mi} \mathbb{1}_{\{\tau_{i-1} \leq \alpha_k < \tau_i\}} \alpha_k. \tag{14}$$

Now,

$$\left(\sum_{k=1}^{K} \sum_{i=1}^{M} g_{mi} \alpha_k \mathbb{1}_{\{\tau_{i-1} \leq \alpha_k < \tau_i\}} \right)^p = \sum_{\mathbf{q} \in \mathcal{Q}} C_{p;\mathbf{q}} \prod_{l=1}^{K} \left(\sum_{i=1}^{M} g_{mi} \alpha_l \mathbb{1}_{\{\tau_{i-1} \leq \alpha_l < \tau_i\}} \right)^{q_l} \tag{15}$$

with $\mathcal{Q}$ being the set of all vectors $\mathbf{q} \in \{0, 1, \ldots, p\}^K$ such that $\sum_{l=1}^{K} q_l = p$, and $C_{p;\mathbf{q}} = \frac{p!}{\prod_{l=1}^{K} q_l!}$ [27, Chapter 23]. Since the α_ls are independent,

$$E\left[h_m^p\right] = \prod_{l=1}^{K} E\left[\left(\sum_{i=1}^{M} g_{mi} \alpha_l \mathbb{1}_{\{\tau_{i-1} \leq \alpha_l < \tau_i\}} \right)^{q_l} \right]. \tag{16}$$

Now,

$$\left(\sum_{i=1}^{M} g_{mi}\alpha_l \mathbb{1}_{\{\tau_{i-1}\le\alpha_k<\tau_i\}}\right)^{q_l} = \sum_{i=1}^{M} g_{mi}^{q_l}\alpha_l^{q_l}\mathbb{1}_{\{\tau_{i-1}\le\alpha_k<\tau_i\}}. \tag{17}$$

Since each α_k is a Rayleigh distributed random variable (r.v.) with variance Ω_k, we can write $E[\alpha_k^p \mathbb{1}_{\{\tau_{i-1}\le\alpha_k<\tau_i\}}]$ as

$$E[\alpha_k^p \mathbb{1}_{\{\tau_{i-1}\le\alpha_k<\tau_i\}}] = \Omega_k^{\frac{p}{2}} f(p;\Omega_k;\tau_{i-1},\tau_i), \tag{18}$$

with

$$f(p;\Omega_k;\tau_{i-1},\tau_i) \triangleq \frac{1}{2^{\frac{p}{2}}}\Gamma\left(1+\frac{p}{2}\right) \left(\gamma_{\text{inc}}\left(\frac{\tau_i^2}{\Omega_k},1+\frac{p}{2}\right)-\gamma_{\text{inc}}\left(\frac{\tau_{i-1}^2}{\Omega_k},1+\frac{p}{2}\right)\right),$$

and $\gamma_{\text{inc}}(x,a) = \frac{1}{\Gamma(a)}\int_0^x e^{-u}u^{a-1}du$ denoting the standard incomplete Gamma function [28].

Thus, pth moment of the effective channel coefficient for the mth bit is given by

$$E[h_m^p] = \sum_{\mathbf{q}\in\mathcal{Q}} C_{p;\mathbf{q}} \prod_{l=1}^{K}\sum_{i=1}^{M} g_{mi}^{q_l}\Omega_k^{\frac{q_l}{2}} f(q_l;\Omega_k;\tau_{i-1},\tau_i). \tag{19}$$

For $p=1$, the above simplifies to

$$E[h_m] = \sum_{k=1}^{K}\Omega_k^{\frac{1}{2}}\sum_{i=1}^{M} g_{mi} f(1;\Omega_k;\tau_{i-1},\tau_i). \tag{20}$$

For $\Omega_k=\Omega\ \forall k$, this further reduces to

$$E[h_m] = K\sqrt{\Omega}\sum_{i=1}^{M} g_{mi} f(1;\Omega;\tau_{i-1},\tau_i). \tag{21}$$

This gives us an analytical expression for $E[h_m]$. For later use, we derive an alternative expression for $E[h_m]$ in Appendix A given by:

$$E[h_m] = \sum_{k=1}^{K} k\sqrt{\Omega}\Pr\{\kappa_m=k\}\sum_{i=1}^{M} g_{mi}\bar{f}(p;\Omega;\tau_{i-1},\tau_i,\tau_{m-1}), \tag{22}$$

where $\Pr\{\kappa_m=k\}$ is the probability that k nodes transmit the mth bit, and

$$\bar{f}(p;\Omega;\tau_{i-1},\tau_i,\tau_{m-1}) = \frac{f(p;\Omega;\tau_{i-1},\tau_i)}{f(0;\Omega;\tau_{m-1},\infty)}. \tag{23}$$

Similarly, for $p=2$, when $\Omega_k=\Omega$ for all k,

$$E[h_m^2] = K\Omega\sum_{i=1}^{M} g_{mi}^2 f(2;\Omega;\tau_{i-1},\tau_i) + K(K-1)\Omega\left(\sum_{i=1}^{M} g_{mi} f(1;\Omega;\tau_{i-1},\tau_i)\right)^2, \tag{24}$$

and consequently,

$$\text{var}(h_m) = K\Omega\left[\sum_{i=1}^{M} g_{mi}^2 f(2;\Omega;\tau_{i-1},\tau_i) - \left(\sum_{m=1}^{M} g_{mi} f(1;\Omega;\tau_{i-1},\tau_i)\right)^2\right]. \tag{25}$$

The mean of the effective channel scales linearly with the number of SNs, and this is a consequence of the coherent combining gain at the FC. Additionally, the variance of the effective channel for the mth bit also scales linearly with the number of SNs. Consequently, its coefficient of variation decays as $\frac{1}{\sqrt{K}}$. Hence, the effective channel coefficient hardens to its mean value as K gets large.

B. Channel Statistics with Estimated CSI at the SNs

The channel fade seen by the kth SN, $\alpha_k e^{j\theta_k}$, is a zero mean complex Gaussian r.v. with variance Ω_k. Due to linear channel estimation at the SNs, the complex valued channel estimate, $\hat{\alpha}_k e^{j\hat{\theta}_k}$, is also Gaussian. With a linear least-squares estimator, we have $E[\hat{\alpha}_k^2] = \hat{\Omega}_k \triangleq \Omega_k\left(1+\frac{1}{\xi_k}\right)$, where $\xi_k = \frac{\mathcal{E}_p\Omega_k}{N_0}$ is the pilot SNR at the kth node. Also, due to the joint Gaussianity of $\alpha_k e^{j\theta_k}$ and $\hat{\alpha}_k e^{j\hat{\theta}_k}$, we can write

$$\alpha_k e^{j\theta_k} = \hat{\beta}_k\hat{\alpha}_k e^{j\hat{\theta}_k} + \tilde{\beta}_k\tilde{\alpha}_k e^{j\tilde{\theta}_k}, \tag{26}$$

where $\hat{\beta}_k = \frac{\xi_k}{1+\xi_k}$ and $\tilde{\beta}_k = \sqrt{\frac{1}{1+\xi_k}}$, also $\tilde{\alpha}_k e^{j\tilde{\theta}_k}$ is a zero mean complex Gaussian r.v. with variance Ω_k, independent of $\hat{\alpha}_k e^{j\hat{\theta}_k}$. Substituting (26) into (14), we obtain $h_m = \hat{h}_m + \tilde{h}_m$, where

$$\hat{h}_m = \sum_{i=1}^{M} g_{mi}\sum_{k=1}^{K}\hat{\beta}_k\hat{\alpha}_k\mathbb{1}_{\{\tau_{i-1}\le\hat{\alpha}_k<\tau_i\}} \tag{27}$$

is the effective DCP channel from the SNs to the FC, and

$$\tilde{h}_m = \sum_{k=1}^{K} g_m(\hat{\alpha}_k)\tilde{\beta}_k v_k. \tag{28}$$

is a random component introduced due to the channel estimation errors at the SNs, which introduces *self noise*, and will be present even in the absence of additive noise at the receiver.

Now, $\hat{h}$ is a weighted sum of Rayleigh distributed random variables. Its pth moment is given by

$$E[\hat{h}_m^p] = \sum_{\mathbf{q}\in\mathcal{Q}} C_{p;\mathbf{q}}\prod_{l=1}^{K}\sum_{i=1}^{M}(\hat{\beta}_l\Omega_l)^{\frac{q_l}{2}} g_{mi}^{q_l} f(q_l;\hat{\beta}_l^{-1}\Omega_l;\tau_{i-1},\tau_i). \tag{29}$$

Consequently,

$$E[\hat{h}_m] = \sum_{k=1}^{K}(\hat{\beta}_k\Omega_k)^{\frac{1}{2}}\sum_{i=1}^{M} g_{mi} f(1;\hat{\beta}_k^{-1}\Omega_k;\tau_{i-1},\tau_i), \tag{30}$$

and

$$E[\hat{h}_m^2] = \left(\sum_{k=1}^{K}\hat{\beta}_k\Omega_k\sum_{i=1}^{M} g_{mi}^2 f(2;\hat{\beta}_k^{-1}\Omega_k;\tau_{i-1},\tau_i) + \sum_{k=1}^{K}\sum_{l=1;l\neq k}^{K}\left(\hat{\beta}_k\sqrt{\Omega_k}\sum_{i=1}^{M} g_{mi} f(1;\hat{\beta}_k^{-1}\Omega_k;\tau_{i-1},\tau_i)\right) \times \left(\hat{\beta}_l\sqrt{\Omega_l}\sum_{i=1}^{M} g_{mi} f(1;\hat{\beta}_l^{-1}\Omega_l;\tau_{i-1},\tau_i)\right)\right). \tag{31}$$

On the other hand, $\tilde{h}_m$ is a weighted sum of zero mean complex Gaussians r.v.s, and will therefore be zero mean

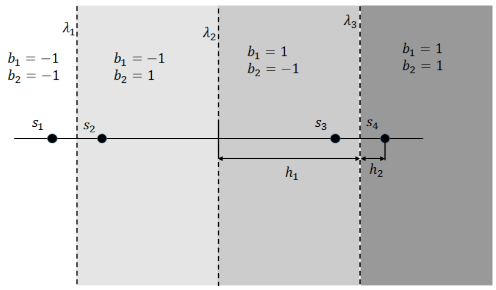

Figure 2. Effective constellation for the proposed system with 2/4 PAM.

complex Gaussian distributed, such that

$$\mathrm{var}(\tilde{h}_m) = \sum_{k=1}^{K} \Omega_k \tilde{\beta}_k^2 \sum_{i=1}^{M} g_{mi}^2 f(0; \hat{\beta}_k^{-1}\Omega_k; \tau_{i-1}, \tau_i). \quad (32)$$

In the next section, we derive recursive expressions for the BER in a DCP-ACS system assuming known channel coefficients. We will use the channel statistics derived in this section for developing blind channel estimation algorithms in Section V and for computing the average BERs under estimated CSI at the FC in Section VI.

IV. BER Computation for Known Channel Coefficients

In this section, we derive recursive expressions for the BER of DCP-ACS systems using both PAM and QAM when the channel instantiation is known at the both the FC and the SNs. The assumption of knowing the channel coefficients allows us to derive recursive expressions for the BER. We then use the channel statistics to derive the average BER performances in Section VI. We first derive the BERs for the 2/4-PAM and 2/4/8 PAM constellations with ACS. This allows us to generalize the results to the $2/4/\ldots/2^M$ case and obtain recursive expressions for the BER. For the purpose of this discussion, we let $P_e^{\text{PAM}}(M, \mathbf{h}, m)$ and $P_e^{\text{QAM}}(2M, \mathbf{h}, m)$ denote the probability of bit error in the mth bit of an M bit PAM ($2M$ bit for QAM) constellation when the effective channel at the FC is $\mathbf{h}$ as defined in (10). Note that the effective channel $\mathbf{h}$ depends on the actual channel coefficients, $\alpha_k e^{j\theta_k}$, and the thresholds $\tau_1, \ldots, \tau_{M-1}$ through (8).

A. BER for 2/4 PAM Constellation

The real part, $y_c[n]$, of the received signal $y[n]$ defined in (9) can be written as

$$y_c[n] = \sqrt{\mathcal{E}_s} h_1 b_1[n] + \sqrt{\mathcal{E}_s} h_2 b_2[n] + w_c[n], \quad (33)$$

where $w_c[n]$ is the real component of the zero mean complex Gaussian noise, such that $w_c[n] \sim \mathcal{N}(0, \frac{N_0}{2})$.

The effective constellation for the signal $y_c[n]$ is illustrated in Fig. 2. It can be seen that the distances of different symbols from the origin can be written in terms of the effective channel coefficients h_1 and h_2, such that $s_1 = -h_1 - h_2$, $s_2 = -h_1 + h_2$, $s_3 = h_1 - h_2$, and $s_4 = h_1 + h_2$. The corresponding decision boundaries can be defined as $\lambda_0 = -\infty$, $\lambda_1 = \frac{s_1+s_2}{2}$, $\lambda_2 = \frac{s_2+s_3}{2}$, $\lambda_3 = \frac{s_3+s_4}{2}$, and $\lambda_4 = \infty$. Using these, we can write the decision rule for the symbol $\hat{s}[n]$ as $\hat{s}[n] = s_p$ if $\lambda_{p-1} \leq y[n] < \lambda_p$.

Since we consider different classes of bits with different levels of error protection, we are interested in deriving the error rates for the individual bits. We therefore derive the BERs for the two bits of a 2/4 PAM system.

Considering the MSB first, it can be observed that an error occurs when the a symbol from the pair (s_1, s_2) is detected as a symbol from the pair (s_3, s_4), or vice versa, while no errors occur in all other cases. Hence, the probability of error in the MSB can be written as

$$\begin{aligned} P_e^{\text{PAM}}(2, \mathbf{h}, 1) = \frac{1}{4} \Big(& Q\left(\sqrt{2|s_1 - \lambda_2|^2 \gamma_{\text{in}}}\right) \\ & + Q\left(\sqrt{2|s_2 - \lambda_2|^2 \gamma_{\text{in}}}\right) + Q\left(\sqrt{2|s_3 - \lambda_2|^2 \gamma_{\text{in}}}\right) \\ & + Q\left(\sqrt{2|s_4 - \lambda_2|^2 \gamma_{\text{in}}}\right)\Big) \end{aligned} \quad (34)$$

where $\gamma_{\text{in}} \triangleq \frac{\mathcal{E}_s}{N_0}$. This can be simplified to

$$\begin{aligned} P_e^{\text{PAM}}(2, \mathbf{h}, 1) = \frac{1}{2} \Big(& Q\left(\sqrt{2|h_1 + h_2|^2 \gamma_{\text{in}}}\right) \\ & + Q\left(\sqrt{2|h_1 - h_2|^2 \gamma_{\text{in}}}\right)\Big). \end{aligned} \quad (35)$$

Next, considering the LSB, it can be seen that there will be an error when the a symbol from the pair (s_1, s_3) is detected as a symbol from the pair (s_2, s_4) or vice versa, whereas there will be no bit error when one symbol from a within pair is detected as the other. Using these facts, the BER for the LSB takes the form

$$\begin{aligned} P_e^{\text{PAM}}(2, \mathbf{h}, 2) = & Q\left(\sqrt{2|h_2|^2 \gamma_{\text{in}}}\right) \\ & + \frac{1}{4}\Big(Q\left(\sqrt{2|h_1 - h_2|^2 \gamma_{\text{in}}}\right) - Q\left(\sqrt{2|h_1 + h_2|^2 \gamma_{\text{in}}}\right) \\ & + Q\left(\sqrt{2|2h_1 + h_2|^2 \gamma_{\text{in}}}\right) - Q\left(\sqrt{2|2h_1 - h_2|^2 \gamma_{\text{in}}}\right)\Big). \end{aligned} \quad (36)$$

Since $h_2 \leq \frac{h_1}{2}$, and both h_1 and h_2 are positive, it can be seen that the BER for the MSB is smaller than that for the LSB. For example, when $\tau = \infty$, (35) reduces to the BER for a simple BPSK with channel h_1, and (36) reduces to 0.5.

B. BER for Generalized-PAM Constellations

The real part of the received signal for a generalized 2/4/8 PAM [17] system can be written as

$$y_c = \sqrt{\mathcal{E}_s} h_1 b_1[n] + \sqrt{\mathcal{E}_s} h_2 b_2[n] + \sqrt{\mathcal{E}_s} h_3 b_3 + w_c[n]. \quad (37)$$

The BER for the MSB therefore takes the form

$$\begin{aligned} P_e^{\text{PAM}}(3, \mathbf{h}, 1) = \frac{1}{4} \Big(& Q\left(\sqrt{2|h_1 + h_2 + h_3|^2 \gamma_{\text{in}}}\right) \\ & + Q\left(\sqrt{2|h_1 - h_2 + h_3|^2 \gamma_{\text{in}}}\right) \\ & + Q\left(\sqrt{2|h_1 + h_2 - h_3|^2 \gamma_{\text{in}}}\right) \\ & + Q\left(\sqrt{2|h_1 - h_2 - h_3|^2 \gamma_{\text{in}}}\right)\Big). \end{aligned} \quad (38)$$

Defining, $\mathbf{h}^{(m)} \triangleq [h_1, \dots, h_m]^T$, $\mathbf{h}_+^{(m)} \triangleq [h_1, \dots, h_m + h_{m+1}]^T$, and $\mathbf{h}_-^{(m)} \triangleq [h_1, \dots, h_m - h_{m+1}]^T$, it can be shown via simple algebraic manipulation that

$$P_e^{\text{PAM}}(3, \mathbf{h}^{(3)}, 1) = \frac{1}{2}(P_e^{\text{PAM}}(2, \mathbf{h}_+^{(2)}, 1) + P_e^{\text{PAM}}(2, \mathbf{h}_-^{(2)}, 1)), \tag{39}$$

and similarly,

$$P_e^{\text{PAM}}(3, \mathbf{h}^{(3)}, 2) = \frac{1}{2}(P_e^{\text{PAM}}(2, \mathbf{h}_+^{(2)}, 2) + P_e^{\text{PAM}}(2, \mathbf{h}_-^{(2)}, 2)). \tag{40}$$

This arises from the fact that the addition of the mth bit to the constellation results in splitting of the constellation points corresponding to the $(m-1)$th bit into two new constellation points, equidistant from the constellation point corresponding to the $(m-1)$th bit and with the same average signal power. The BERs for the lth most significant bit in an m-bit ($l < m$) PAM constellation can therefore be recursively computed as:

$$P_e^{\text{PAM}}(m, \mathbf{h}^{(m)}, l) = \frac{1}{2}(P_e^{\text{PAM}}(m-1, \mathbf{h}_+^{(m-1)}, l) + P_e^{\text{PAM}}(m-1, \mathbf{h}_-^{(m-1)}, l)). \tag{41}$$

To obtain the BER of the LSB, we note that the pth symbol, s_p, will be $s_p = \sum_{m=1}^{M} h_m b_{p,m}$. The LSB is in error whenever s_p is detected as s_{p+l} where l is odd and s_{p+l} lies in the constellation, and there is no error when s_p is detected as s_{p+l}, with l being even and s_{p+l} lying in the constellation. Defining $\lambda_q = \frac{1}{2}(s_q + s_{q+1})$, $1 \leq q \leq 2^M$ as the qth decision boundary with $\lambda_0 = -\infty$ and $\lambda_M = \infty$, we can write the probability of s_p being detected as $s_{p'}$ as

$$P(s_p \to s_{p'}) = Q\left(\sqrt{2|s_p - \lambda_{p'-1}|^2 \gamma_{\text{in}}}\right). \tag{42}$$

Letting $\mathbf{b}_p \in \{-1, +1\}^M$ as the bit pattern corresponding to the pth constellation symbol we can write $s_p = \mathbf{h}^T \mathbf{b}_p$, consequently $\lambda_q = \mathbf{h}^T \frac{(\mathbf{b}_q + \mathbf{b}_{q+1})}{2}$. Defining $\boldsymbol{\psi}_{p,q} \triangleq \mathbf{b}_p - \frac{(\mathbf{b}_q + \mathbf{b}_{q+1})}{2}$, we can write the above as

$$P(s_p \to s_q) = Q\left(\sqrt{2|\mathbf{h}^T \boldsymbol{\psi}_{p,q-1}|^2 \gamma_{\text{in}}}\right). \tag{43}$$

Using the fact that a bit error occurs if and only if $(p-q)$ is an odd number, we can write,

$$P_e^{\text{PAM}}(m, \mathbf{h}^{(m)}, m) = \frac{1}{2^M} \sum_{p=1}^{2^M - 1} \sum_{q=1; q \neq p}^{2^M} P(s_p \to s_q). \tag{44}$$

This can be shown to take the form

$$P_e^{\text{PAM}}(m, \mathbf{h}^{(m)}, m) = \frac{1}{2^M} \sum_{p=1}^{2^M} \sum_{q=1; q \neq p}^{2^M - 1} (-1)^{p-q} \text{sign}(p-q) Q\left(\sqrt{2|\mathbf{h}^T \boldsymbol{\psi}_{p,q-1}|^2 \gamma_{\text{in}}}\right) \tag{45}$$

where $\text{sign}(x) = 1$, if $x > 0$, $\text{sign}(x) = -1$ if $x < 0$, and $\text{sign}(x) = 0$ if $x = 0$. Thus, we have obtained recursive expressions for computing the probabilities of bit error in different bits for an M-bit PAM.

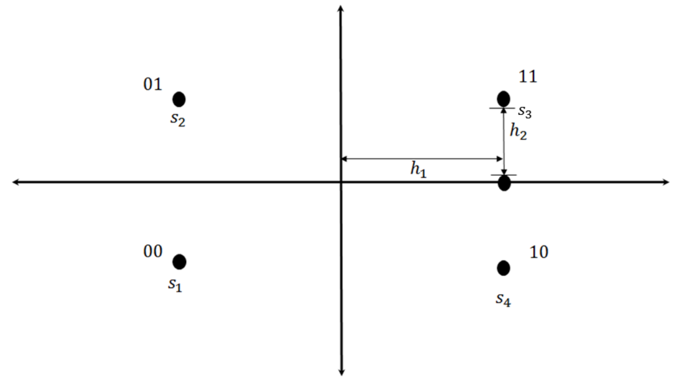

Figure 3. Effective constellation for the proposed system when different nodes choose from BPSK/QPSK based on the channel state.

C. BER for 2M-bit QAM Constellations

We first derive the BER for a BPSK/QPSK constellation as shown in Fig 3. Here, the SNs transmit only the MSB using a BPSK constellation if the channel gain is below the threshold τ_1, and transmit both the MSB and LSB using a QPSK constellation otherwise. We can write $y_s[n]$ and $y_c[n]$, the real and imaginary parts of the received signal, respectively, as

$$\begin{aligned} y_c[n] &= \sqrt{\mathcal{E}_s} h_1 b_1[n] + w_c[n] \\ y_s[n] &= \sqrt{\mathcal{E}_s} h_2 b_2[n] + w_s[n]. \end{aligned} \tag{46}$$

where $w_c[n]$ and $w_s[n]$ are both AWGNs with variance $N_0/2$.

Therefore, the in-phase and quadrature components of a BPSK/QPSK constellation can be analyzed separately, resulting in the BER expressions

$$\begin{aligned} P_e^{\text{QAM}}(2, \mathbf{h}, 1) &= Q\left(\sqrt{2|h_1|^2 \gamma_{\text{in}}}\right) \\ P_e^{\text{QAM}}(2, \mathbf{h}, 2) &= Q\left(\sqrt{2|h_2|^2 \gamma_{\text{in}}}\right). \end{aligned} \tag{47}$$

Similarly, the real and imaginary components of a $2M$ bit QAM constellation can be written as

$$\begin{aligned} y_c[n] &= \sum_{m=1}^{M} h_{2m-1} \sqrt{\mathcal{E}_s} b_{2m-1}[n] + w_c[n], \\ y_s[n] &= \sum_{m=1}^{M} h_{2m} \sqrt{\mathcal{E}_s} b_{2m}[n] + w_s[n]. \end{aligned} \tag{48}$$

We can therefore write recursive expressions for the BER as:

$$P_e^{\text{QAM}}(2m, \mathbf{h}_c^{(2m)}, 2l) = \frac{1}{2}(P_e^{\text{QAM}}(2m-2, \mathbf{h}_{c,+}^{(2m-2)}, 2l) + P_e^{\text{QAM}}(2m-2, \mathbf{h}_{c,-}^{(2m-2)}, 2l)), \tag{49}$$

and

$$P_e^{\text{QAM}}(2m, \mathbf{h}_s^{(2m)}, 2l-1) = \frac{1}{2}(P_e^{\text{QAM}}(2m-2, \mathbf{h}_{s,+}^{(2m-2)}, 2l-1) + P_e^{\text{QAM}}(2m-2, \mathbf{h}_{s,-}^{(2m-2)}, 2l-1)). \tag{50}$$

where $l < m$, $\mathbf{h}_c^{(2m)} = [h_1, h_3, \dots, h_{2m-1}]^T$, $\mathbf{h}_s^{(2m)} = [h_2, h_4, \dots, h_{2m}]^T$, $\mathbf{h}_{c,+}^{(2m)} = [h_1, h_3, \dots, h_{2m-1} + h_{2m+1}]^T$, $\mathbf{h}_{s,+}^{(2m)} = [h_2, h_4, \dots, h_{2m} + h_{2m+2}]^T$, $\mathbf{h}_{c,-}^{(2m)} = [h_1, h_3, \dots, h_{2m-1} - h_{2m+1}]^T$ and

$\mathbf{h}_{s,-}^{(2m)} = [h_2, h_4, \ldots, h_{2m} - h_{2m+2}]^T$. Similarly, defining $\mathbf{b}_{2p-1}$ and $\mathbf{b}_{2p}$ as the M-bit patterns corresponding to s_{2p-1} and s_{2p}, the BER expression for the LSB in the in-phase and quadrature components become

$$P_e^{\text{QAM}}(2m, \mathbf{h}^{(m)}, 2m-1) = \frac{1}{2^M} \sum_{p=1}^{2^M} \sum_{q=1; q \neq p}^{2^M - 1} (-1)^{p-q} \times \text{sign}(p-q) Q\left(\sqrt{2|\mathbf{h}_c^{(2m)T} \boldsymbol{\psi}_{2p-1,2q-3}|^2 \gamma_{\text{in}}}\right),$$

$$P_e^{\text{QAM}}(2m, \mathbf{h}^{(m)}, 2m) = \frac{1}{2^M} \sum_{p=1}^{2^M} \sum_{q=1; q \neq p}^{2^M - 1} (-1)^{p-q} \times \text{sign}(p-q) Q\left(\sqrt{2|\mathbf{h}_s^{(2m)T} \boldsymbol{\psi}_{2p,2q-2}|^2 \gamma_{\text{in}}}\right), \quad (51)$$

where $\boldsymbol{\psi}_{2p-i,2q-2-i} = \mathbf{b}_{2p-i} - \frac{(\mathbf{b}_{2q-i} + \mathbf{b}_{2q-i+2})}{2}$, $i \in \{0, 1\}$.

In this section, we derived recursive expressions to calculate the BERs for different bits in an DCP-ACS system using PAM and rectangular QAM constellations. All the BER expressions derived here are conditioned on the channel gains between the SNs and the FC. These expressions need to be averaged over the channel statistics to obtain the BER for the proposed system. Also, recall that, in our setup, the SNs do not transmit pilots. Therefore, the FC has to estimate CSI blindly from the data symbols in order to perform data detection. The error in estimation of the CSI at the FC can result in a degradation of the BER. In the next section, we address the estimation of the CSI at the FC, and in Section VI, we derive the expressions for the average BER over the channel realizations.

V. Blind Channel Estimation Techniques

It was shown above that it is possible to achieve unequal error protection in DCP systems by allowing different nodes to transmit from different symbol constellations based on the estimated channel gains. However, the BER expressions derived previously assumed perfect knowledge of the channel at the FC. Since the SNs do not use forward link training, the channel is unknown at the FC. It was shown in our previous work [9], [25] that the structure induced by the DCP channel allows for blind channel estimation at the FC in case all the SNs transmit symbols from the same constellation. In this section, we develop three blind channel estimation techniques for DCP systems employing ACS at the SNs.

A. Clustering Based Decoding

The real and imaginary parts of the signal received at the FC for a $2M$-bit QAM constellation can be written as

$$y_c[n] = \sum_{m=1}^{M} \hat{h}_{2m-1} \sqrt{\mathcal{E}_s} b_{2m-1} + z_c[n] + w_c[n], \quad (52)$$

$$y_s[n] = \sum_{m=1}^{M} \hat{h}_{2m} \sqrt{\mathcal{E}_s} b_{2m} + z_s[n] + w_s[n]. \quad (53)$$

If we define $z[n] \triangleq \sum_{m=1}^{M} \tilde{h}_{2m-1} \sqrt{\mathcal{E}_s} b_{2m-1}[n] + j\tilde{h}_{2m} \sqrt{\mathcal{E}_s} b_{2m}[n]$ as the self noise caused due to CSI imperfections at the SNs, then $z_c[n]$ and $z_s[n]$ in (52) and (53) are the real and imaginary parts of $z[n]$. Note that the channel coefficients, $\hat{h}_m$, are real positive numbers, due to the co-phased transmissions by the SNs and $b_m[n]$s take values from the binary set ± 1. Defining $\mathcal{B}^M \triangleq \{-1, 1\}^M$, we can define the symbol constellations on the real and imaginary axes as $\mathcal{S}_c \triangleq \{\hat{\mathbf{h}}_c^T \mathbf{b} : \mathbf{b} \in \mathcal{B}^M\}$, and $\mathcal{S}_s \triangleq \{\hat{\mathbf{h}}_s^T \mathbf{b} : \mathbf{b} \in \mathcal{B}^M\}$, respectively. The symbols received over the in-phase and the quadrature components can therefore be seen as versions of symbols drawn from these constellations corrupted by self noise and AWGN. Consequently, both the received $y_c[n]$ and $y_s[n]$ can each be classified into 2^M distinct clusters. Clustering of both the in-phase and the quadrature streams can be achieved using standard unsupervised clustering schemes, such as one of the variants of the K-means algorithm [29], [30]. In our work, we use the fuzzy K-means algorithm [31]. We write the sorted cluster centers of $y_c[n]$ and $y_s[n]$ respectively as the vectors $\mathbf{c}_c$ and $\mathbf{c}_s$ with $\mathbf{c}_i = [c_{i,1}, c_{i,2}, \ldots, c_{i,2^M}]^T$; $i = \{c, s\}$ such that $c_{i,1} < c_{i,2} < \cdots < c_{i,2^M}$.

Since the channel coefficients $\hat{h}_m$ are real and positive numbers, the symbols of the resulting constellations $s_{i,l}$, $i \in \{c, s\}$, and $l \in 1, \ldots, 2^M$ can also be sorted as $s_{c,1} = -\sum_{m=1}^{M} \hat{h}_{2m-1} < \cdots < s_{c,2^M} = \sum_{m=1}^{M} \hat{h}_{2m-1}$, and $s_{s,1} = -\sum_{m=1}^{M} \hat{h}_{2m} < \cdots < s_{s,2^M} = \sum_{m=1}^{M} \hat{h}_{2m}$. Since the cluster centers of the real and imaginary parts of the received signals correspond to these constellation points,

$$\mathbf{c}_i = \mathbf{s}_i + \boldsymbol{\nu}_i; \; i \in \{c, s\}, \quad (54)$$

where $\boldsymbol{\nu}_i$ is the residual noise arising from the AWGN and the self noise of the DCP-ACS system.

Note that the individual bits can be recovered by simply mapping each received symbol to a cluster center, and using the bit sequence corresponding to that cluster center.

Defining $\mathbf{A}$ as the $M \times 2^M$ matrix containing all the elements of $\mathcal{B}^M$, we can write the least squares estimate $\bar{\mathbf{h}}_i$ of $\hat{\mathbf{h}}_i$ as

$$\bar{\mathbf{h}}_i = \mathbf{A}^\dagger \mathbf{c}_i; \; i \in \{c, s\}, \quad (55)$$

where $\mathbf{A}^\dagger$ represents the Moore-Penrose pseudoinverse of the matrix $\mathbf{A}$. With cluster based decoding, the data bits are detected using (54), and the channel estimate is obtained as a byproduct of (55). This estimate is used for performance comparison with the successive decoding and iterative estimation and decoding schemes, which we describe next.

B. Successive Decoding

Consider the first terms in the summations in (52) and (53). Let $y_1[n] \triangleq y_c[n]$ and $y_2[n] \triangleq y_s[n]$. We can write

$$y_1[n] = \sqrt{\mathcal{E}_s} h_1 b_1[n] + v_1[n] \quad (56)$$

$$y_2[n] = \sqrt{\mathcal{E}_s} h_2 b_2[n] + v_2[n], \quad (57)$$

where $v_1[n]$ and $v_2[n]$ are the cumulative effects of the lower priority bits and the additive noise. Also, by design,

$$|h_1 b_1[n]| > \left| \left\{ \sum_{i=2}^{M} h_{2m-1} b_{2m-1}[n] \right\} \right| \quad (58)$$

and

$$|h_2 b_2[n]| > \left| \left\{ \sum_{i=2}^{M} h_{2m} b_{2m}[n] \right\} \right|. \tag{59}$$

Therefore, in the absence of additive noise, $y_i[n] > 0$ for $b_i[n] = 1$ and $y_i[n] < 0$ for $b[n] = -1$, $i \in \{1, 2\}$. Hence, the ML estimates, $\bar{b}_i[n]$, of the bits $b_i[n]$, $i \in \{1, 2\}$, can be obtained by taking the signs of the signal $y_i[n], i \in \{1, 2\}$. Following this, the modified K-means based blind channel estimation algorithm presented in [25] can be used to iteratively compute the estimates $\bar{h}_i$ of $\hat{h}_i$. These can then be used to define the residuals $y_3[n] = y_1[n] - \bar{h}_1 \bar{b}_1[n]$, and $y_4[n] = y_2[n] - \bar{h}_2 \bar{b}_2[n]$, which and in turn be used to detect $b_3[n]$ and $b_4[n]$ and obtain the estimates for $\hat{h}_3$ and $\hat{h}_4$. This process of successive decoding and cancellation can be used to detect all the bits received at the FC, as well as obtain the estimates of all the associated channel coefficients.

C. Iterative Channel Estimation and Decoding

Our starting point is the signal $y[n]$ in (13):

$$y[n] = \sum_{m=1}^{M} h_{2m-1} \sqrt{\mathcal{E}_s} b_{2m-1}[n] + j h_{2m} \sqrt{\mathcal{E}_s} b_{2m}[n] + w[n] \tag{60}$$

where $h_m = \hat{h}_m + \tilde{h}_m$ is the complex valued channel gain for the mth bit that includes the effect of both DCP and self noise. Ideally, knowledge of the true effective DCP channels, h_m, would result in superior data detection performance compared to estimating $\hat{h}_m$ and decoding the data by assuming $\hat{h}_m$ as the channel coefficient. However, estimating h_m at the FC requires training symbols, which are not available at the FC. On the other hand, by design, the phase of h_m is close to zero (and equals zero in the absence of channel estimation errors at the SNs) [7]. We can exploit this to iteratively detect the data and estimate the channel using the detected data as pilot symbols, until convergence, as explained next.

Stacking N_d consecutive received symbols as a row vector $\mathbf{y}$, we can write $\mathbf{y} = \mathbf{h}^T \mathbf{B} + \mathbf{w}$, where $\mathbf{h} \in \mathbb{C}^{2M \times 1}$ is the effective channel vector, $\mathbf{B} \in \mathbb{C}^{2M \times N}$ is the transmitted data matrix with the nth column, $\mathbf{b}[n]$, representing the nth transmitted symbol, and is expressed as $\mathbf{b}[n] = [b_1[n], jb_2[n], \ldots, b_{2M-1}[n], jb_{2M}[n]]^T$. The joint channel estimation and data detection problem to determine the ML estimates $\bar{\mathbf{B}}$ and $\bar{\mathbf{h}}$ of $\mathbf{B}$ and $\mathbf{h}$ can now be written as

$$(\bar{\mathbf{h}}, \bar{\mathbf{B}}) = \arg \min_{\mathbf{B}, \mathbf{h}} \|\mathbf{y} - \mathbf{h}^T \mathbf{B}\|. \tag{61}$$

Since the data matrix and the channel vectors are independent, we can minimize the above expression independently w.r.t. $\mathbf{B}$ and $\mathbf{h}$, resulting in the sub-problems

$$\bar{\mathbf{h}} = \arg \min_{\mathbf{h}} \|\mathbf{y} - \mathbf{h}^T \bar{\mathbf{B}}\|, \tag{62}$$

$$\bar{\mathbf{b}}[n] = \arg \min_{\mathbf{b}[n]} \|y[n] - \mathbf{h}^T \mathbf{b}[n]\|. \tag{63}$$

The optimization problem in (62) is a standard least squares problem, whose solution is

$$\bar{\mathbf{h}} = (\mathbf{y} \bar{\mathbf{B}}^{\dagger})^T. \tag{64}$$

Table I

COMPARISON OF COMPUTATIONAL COMPLEXITIES OF DIFFERENT APPROACHES FOR DCP-ACS.

Technique	Computational Complexity
Clustering Based Decoding	$\mathcal{O}(N_d 2^{2M})$
Successive Decoding	$\mathcal{O}(MN_d)$
Iterative Channel Estimation and Decoding	$\mathcal{O}(MN_d^2) + \mathcal{O}(N_d 2^{2M})$

Equation (63) is a symbol detection problem with a known vector channel and can be solved via a search over the symbol space $\mathcal{B}^K$. It can be seen that both these problems can be solved iteratively, and since the objective function is convex in both $\mathbf{h}$ and $\mathbf{B}$, the iterative solution of (62) and (63) is guaranteed to converge to a local minimum. The initial solution to these equations can be obtained using either clustering based decoding or successive decoding.

D. Comparison of Blind Channel Estimation Algorithms

We first compare the computational complexities of the three algorithms. For this purpose, we consider a total of N_d symbols each containing a maximum of $2M$ bits, M transmitted over the in-phase constellation and M over quadrature, resulting in 2^M points in both I and Q PAM constellations. First, the clustering based algorithm uses the fuzzy K-means algorithm to determine the cluster centers. Hence, its computational complexity is of the order of the fuzzy K-means algorithm [31]. Therefore, this has a complexity of order $\mathcal{O}(N_d 2^{2M})$ for both the in-phase and the quadrature components. Second, the successive decoding based detection requires thresholding of each bit followed by $2N_d$ complex multiplications for each step, resulting in a total complexity of order $\mathcal{O}(MN_d)$ for both the in-phase and quadrature components. Third, for the iterative channel estimation and decoding technique, since $\mathbf{h}$ is a length $2M$ vector and $\mathbf{B}$ is a $2M \times N_d$ matrix, the computational cost for equation (64) is $\mathcal{O}(MN_d^2)$ and that for (63) is $\mathcal{O}(N_d 2^{2M})$. Therefore, the successive decoding based detection technique has the least computational complexity, followed by the clustering based decoding technique, and iterative minimization based approach, has the maximum computational complexity. A summary of the computational complexities of the three different approaches considered in this paper is provided in Table I.

Recall that the clustering based decoding, unlike successive decoding and iterative channel estimation and decoding, does not use the detected bits for channel estimation. This results in poorer channel estimates at the FC. On the other hand, it does not suffer from the effects of error propagation.

Figure 4 plots the normalized MSE $\frac{\|\mathbf{h} - \bar{\mathbf{h}}\|^2}{\|\mathbf{h}\|^2}$ of the different channel estimation algorithms at different data SNRs and for different numbers of data symbols. It can be observed that the NMSEs for the clustering based decoding and the successive decoding approaches saturate, whereas that for the iterative minimization approach decreases with increase in the data SNR. Also, due to the fact that the effect of error propagation is high at lower SNRs, the NMSE improves only marginally with an increase in the number of transmitted

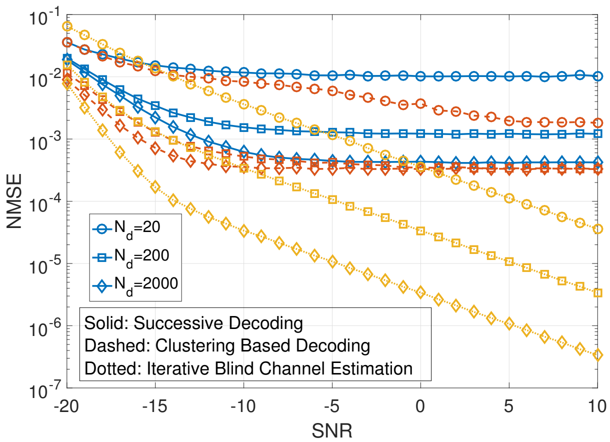

Figure 4. NMSE comparison of channel estimation algorithms for different numbers of data symbols as a function of the data SNR, with 20 SNs.

symbols. However, at moderate to high SNRs, with low error rates, the effects of error propagation become negligible.

VI. Performance Impact of Channel Estimation

In Section IV, we assumed that perfect CSI is available at both the SNs as well as at the FC to simplify the BER computations. Additionally, the expressions derived in Section IV are conditioned on the channel instantiations. However, in a practical system, the CSI available at both the SNs and the fusion center could be imperfect due to the channel estimation errors. In this section, we first characterize the effect of imperfect CSI. Following this, we account for the randomness of the channel coefficients and develop approximate BER expressions for the proposed DCP-ACS system.

A. Effect of Estimated CSI

Let us consider a $2M$ bit QAM system with channel estimates $\hat{\alpha}_k e^{j\hat{\theta}_k}$ available at the SNs. Substituting the true channel in terms of the channel estimate and the estimation error into (13), the received signal becomes

$$y[n] = \sum_{m=1}^{M} (\hat{h}_{2m-1} + \tilde{h}_{2m-1}) b_{2m-1}[n] + j(\hat{h}_{2m} + \tilde{h}_{2m}) b_{2m}[n] + w[n], \quad (65)$$

It was shown in the previous section that for moderate to high SNRs, the normalized MSE of the blindly estimated channel at the FC is less than 10^{-2} even for a small number of data symbols. Therefore, FC can be assumed to know h_m accurately. However, since h_m now consists of two independent components, we can write, $E[h_m] = E[\hat{h}_m] + E[\tilde{h}_m] = E[\hat{h}_m]$ and $E[|h_m|^2] = E[\hat{h}_m^2] + E[|\tilde{h}_m|^2]$, where the modulus is not required for the first term as it is real and positive due to the phase compensation by the nodes. For i.i.d. channels, these can be written as

$$E[h_m] = K(\hat{\beta}\Omega)^{1/2} \sum_{i=1}^{M} g_{mi} f(1; \hat{\beta}^{-1}\Omega, \tau_{i-1}, \tau_i), \quad (66)$$

and

$$E[|h_m|^2] = K\Omega \left(\sum_{i=1}^{M} g_{mi}^2 f(2; \Omega; \tau_{i-1}, \tau_i) + (K-1) \times \left(\sum_{i=1}^{M} g_{mi} f(1; \Omega; \tau_{i-1}, \tau_i) \right)^2 + \tilde{\beta}^2 f(0; \hat{\beta}^{-1}\Omega; \tau_{i-1}, \tau_i) \right).$$

We use the above to derive a closed-form approximate expression for the BER in the next subsection.

B. Effect of Channel Fading

In Section IV, we derived the BERs of the DCP-ACS system as a function of the effective channel coefficients h_m, that in turn are functions of the thresholds $\tau_0, \ldots, \tau_M$. The average BERs for different bits can therefore be determined in terms of the thresholds by averaging the BERs over all the realizations of the channel coefficients. Defining $\boldsymbol{\tau} = [\tau_0, \ldots, \tau_{2M}]^T$, we can write the average BER as

$$\bar{P}_e^{\text{QAM}}(2M, m; \boldsymbol{\tau}) = E_{\mathbf{h}}[P_e^{\text{QAM}}(2M, \mathbf{h}, m)]. \quad (67)$$

Letting

$$R(\boldsymbol{\tau}, \boldsymbol{\psi}_{p,q-1}, \gamma_{\text{in}}) \triangleq E_{\mathbf{h}} \left[Q\left(\sqrt{2|\mathbf{h}^T \boldsymbol{\psi}_{p,q-1}|^2 \gamma_{\text{in}}} \right) \right], \quad (68)$$

we get

$$\bar{P}_e^{\text{QAM}}(2M, m; \boldsymbol{\tau}) = \frac{1}{2^M} \sum_{p=1}^{2^M} \sum_{q=1}^{2^M-1} (-1)^{p-q} \times \text{sign}(p-q) R(\boldsymbol{\tau}, \boldsymbol{\psi}_{p,q-1}, \gamma_{\text{in}}). \quad (69)$$

In order to compute $R(\boldsymbol{\tau}, \boldsymbol{\psi}_{p,q-1}, \gamma_{\text{in}})$, if the channels between the nodes and the FC are i.i.d. distributed, then the coefficient of variation of the effective channel scales inversely with $\sqrt{K}$, resulting in channel hardening [32]. Therefore, if k_m out of K nodes transmit the mth bit, then h_m can be approximated as the function $\dot{h}(k_m)$ such that

$$\dot{h}_m(k_m) = k_m \sqrt{\hat{\beta}\Omega} \sum_{i=1}^{M} g_{mi} \bar{f}(p; \hat{\beta}^{-1}\Omega, \tau_{i-1}, \tau_i, \tau_{m-1}). \quad (70)$$

where $\bar{f}(.; ., ., .)$ is defined in (23). However, the number of nodes transmitting the mth bit, k_m, is a random variable determined by the instantaneous channel, and therefore the average BER can be obtained by averaging over the number of nodes transmitting the mth bit.

The vector $\mathbf{h}$ can be written as a function $\dot{\mathbf{h}}(\boldsymbol{k})$ of the vector $\boldsymbol{k} = [k_1, k_2, \ldots, k_{2M}]$, with $k_{i+1} \leq k_i$. Letting $P_\kappa(\boldsymbol{k})$ denote the probability of the number of nodes transmitting the mth bit being equal to the corresponding entry of $\boldsymbol{k}$, we can write

$$R(\boldsymbol{\tau}, \boldsymbol{\psi}_{p,q-1}; \gamma_{in}) = \sum_{\boldsymbol{k}} P_\kappa(\boldsymbol{k}) Q\left(\sqrt{|\dot{\mathbf{h}}^T(\boldsymbol{k}) \boldsymbol{\psi}_{p,q-1}|^2 \gamma_{\text{in}}} \right). \quad (71)$$

For a two bit system, it can be seen that $k_1 = N$ with probability 1. Hence, the probabilities $P_{\boldsymbol{\kappa}}(\boldsymbol{k}_2)$ can be calculated as $P_{\boldsymbol{\kappa}}(k_2) = \binom{K}{k_2} f^{k_2}(0; \hat{\beta}^{-1}\Omega; \tau_1, \infty) f^{K-k_2}(0; \hat{\beta}^{-1}\Omega; 0, \tau_1)$.

C. Channel Corruption

The above discussion as well as the blind channel estimation algorithms discussed previously are based on fact that the phases of the channel coefficients are close to zero with high probability. However, the perturbations introduced by $\tilde{h}_m$ can occasionally cause the phase of the effective channel to exceed half the rotational symmetry of the constellation being used. This phenomenon, termed as *channel corruption* [25], results in catastrophic errors in the detection of the data bits. In the event of a corruption of the effective channel for a specific bit position, all the corresponding data bits are likely to be detected incorrectly, making the probability of bit error close to unity. However, it was shown in Section V that in the absence of channel corruption, the blind channel estimation algorithms can estimate the true channel with high fidelity. In view of this, the overall error event for the mth bit, $\bar{P}_b^{QAM}(m, 2M; \boldsymbol{\tau})$, can be approximated as the sum of two terms corresponding to the probability of channel corruption and the bit error rate due to additive noise in the absence of channel corruption as follows:

$$\bar{P}_b^{QAM}(m, 2M; \boldsymbol{\tau}) \approx P_{c,m} + (1 - P_{c,m})\bar{P}_e^{\mathrm{QAM}}(m, 2M; \boldsymbol{\tau}), \tag{72}$$

where $P_{c,m}$ is the probability of channel corruption for the mth bit, and $\bar{P}_e^{\mathrm{QAM}}(m, 2M; \boldsymbol{\tau})$ is the probability of error in the lth bit with perfect CSI at the FC. The probability of channel corruption in a DCP system has been derived in in [25], and using that analysis, it can be shown that

$$P_{c,m} \approx Q\left(\frac{\mu_{R,m}}{\sigma_{R,m}}\right) + 2Q\left(\frac{\mu_{R,m}}{\sqrt{\sigma_{I,m}^2 + \sigma_{R,m}^2}}\right) \times \left(1 - Q\left(\frac{\mu_{R,m}}{\sigma_{R,m}}\right)\right), \tag{73}$$

where, $\mu_{R,m} = E[\hat{h}_m]$, $\sigma_{R,m}^2 = \mathrm{var}(\hat{h}_m) + \mathrm{var}(\Re\{\tilde{h}_m\})$, and $\sigma_{I,m}^2 = \mathrm{var}(\Im\{\tilde{h}_m\})$. The moments of $\hat{h}_m$ and $\tilde{h}_m$ derived in Section III can be used to obtain the probability of channel corruption for the mth bit. Plugging these into (72), the BER for the proposed DCP system can be obtained in terms of channel statistics and the threshold vector $\boldsymbol{\tau}$.

D. Choice of the Threshold Vector

In the preceding discussion, the probabilities of error were derived in terms the data/pilot SNRs and the threshold vector, $\boldsymbol{\tau}$. In a practical system, one may wish to choose $\boldsymbol{\tau}$, ξ and γ_{in} based on the required BERs for the different bits given the values of data and pilot SNRs. However, as seen from (20) and (71), the probability of error is a highly nonlinear function of the channel vector $\mathbf{h}$, that is further a nonlinear function of $\boldsymbol{\tau}$. Therefore, the optimization of $\boldsymbol{\tau}$ will have to be performed using numerical methods. The multivariate bisection method [33] is a good approach to this end, since the probability of error of different priority bits is a monotonic function of $\boldsymbol{\tau}$.

VII. Simulation Results

In this section, we use numerical results obtained using Monte Carlo simulation experiments to substantiate the analytical expressions derived previously and to compare the performance of the different channel estimation and data detection schemes.

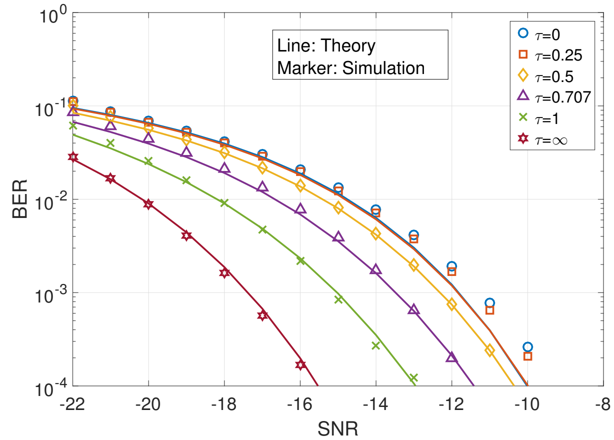

Figure 5. Probability of error in the MSB versus the data SNR for different values of the threshold τ in a 2/4 PAM DCP-ACS system.

We assume that the FC transmits 10 training symbols followed by N_d data symbols from the SNs to the FC using DCP with ACS. Simulations are then carried out for different values of data SNRs, different constellation hierarchies, etc. The pilot SNR is assumed to be fixed at 10 dB unless otherwise specified. The probabilities of symbol error are obtained by averaging over $10,000$ independent channel realizations. Recall that our goal in this paper is to provide different levels of error protection to different data streams. That is, by design, the bit error rate across different streams is different. Therefore, the overall bit error rate plot is not important for our setup, and is not considered here.

In Fig. 5, the error rate of the MSB in a DCP-ACS system selecting between 2 PAM and 4 PAM constellations is plotted as a function of the data SNR. Here, the iterative minimization based scheme derived in Section V is used for joint channel estimation and data detection. The simulated performance of the joint channel estimation and data detection schemes is in close agreement with the theoretical approximations. It is also observed that increasing the transmission threshold for the second bit, τ, from 0 to 1 improves the BER for the MSB by approximately 3 dB at a BER of 10^{-3}. Increasing τ to ∞, that is, always transmitting BPSK, results in a further 2 dB improvement in the BER of the MSB.

In Fig. 6, the BER of the LSB for the system considered in Fig. 5 is plotted. The simulated performance of the joint channel estimation and data detection scheme is again in close agreement with the theoretical approximations. In this case, the BER degrades by approximately 6 dB as τ is varied from 0 to 1. Thus, the use of ACS can lead to a differentiation of about 3 to 6 dB in the BER of the MSB and the LSB. Further increasing the threshold, τ to ∞ results in a BER of 0.5 for the regardless of the transmit SNR, which is expected.

In Figs. 7 and 8, the BER of the MSB and LSB for a DCP-ACS system with the SNs transmitting from either BPSK or QPSK is plotted. As τ changes from 0 to 1, the BER for the MSB and the LSB improves and degrades

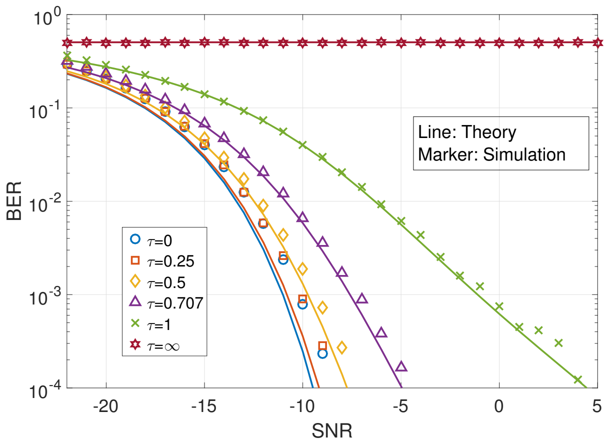

Figure 6. Probability of error in the LSB versus the data SNR for different values of the threshold τ in a 2/4 PAM DCP-ACS system.

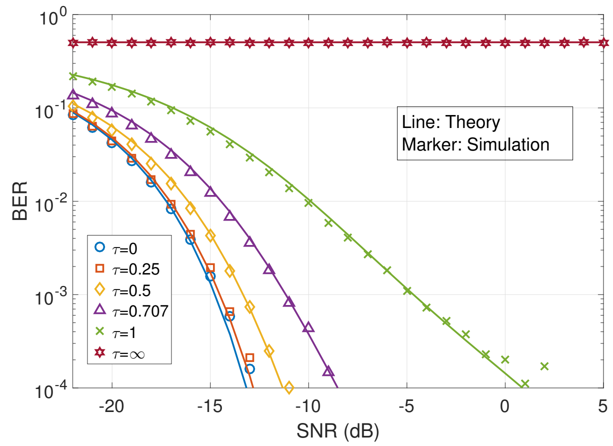

Figure 8. Probability of error in the LSB versus the data SNR for different values of the threshold τ in a BPSK/QPSK DCP-ACS system.

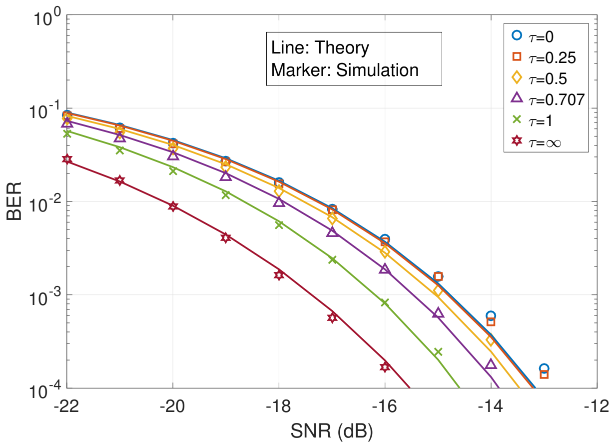

Figure 7. Probability of error in the MSB versus the data SNR for different values of the threshold τ in a BPSK/QPSK DCP-ACS system.

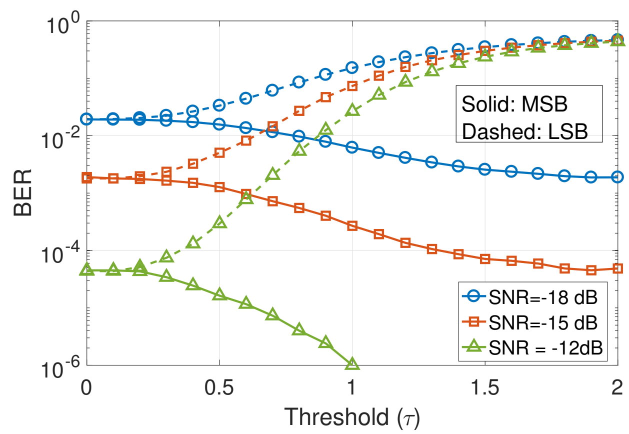

Figure 9. Probability of error versus the threshold τ in for different values of the data SNR for both bits of a BPSK/QPSK DCP-ACS system.

by 2 dB and 10 dB respectively. Yet again, the results of the simulation experiments are in close agreement with the theoretical approximations derived in (70).

In Fig. 9, we plot the BER of the MSB and LSB for a DCP-ACS system with the SNs transmitting from either BPSK or QPSK against the threshold τ. It is observed that by suitably selecting the threshold, τ, the BERs of the higher and lower priority bits of a BPSK/QPSK system can be varied by as much as two orders of magnitude.

In Fig. 10, the BER of the LSB for the system considered in Fig. 5 is plotted for $\tau = 0.707$ and different number of SNs. The channel hardening based approximations are found to be accurate even for 10 SNs. In Fig. 11, the BER of both the bits of a 2/4 PAM system is plotted for different levels of pilot SNR, ξ, taken as a function of the total data SNR, $K\gamma_{\text{in}}$. A pilot SNR boosting of 6 to 9 dB above the total data SNR results in a BER close to that with perfect CSI at the SNs. Also, a constant pilot SNR of 10 dB results in a BER almost identical to that with perfect CSI at the SNs across the data SNR range considered.

We plot the BER of the second (middle) bit in a 2/4/8 QAM system in Fig. 12. This being a rectangular constellation, the MSB is the only bit transmitted on the in-phase component, whereas the two lower order bits are sent over the quadrature carrier using a 2/4 PAM constellation. It is observed that different BER patterns for the second bit can be obtained by appropriately selecting the thresholds τ_1 and τ_2.

VIII. Conclusions

In this work, we showed that using distributed, autonomous constellation selection at different SNs leads to unequal error protection for different bit streams in a DCP based system. We derived the statistics of the effective channel to show that the effective DCP channel concentrates around its mean as the number of SNs gets large. We then used the properties of the effective DCP channels to propose three algorithms for joint data detection and channel estimation at the FC. We developed recursive expressions to evaluate the BER, and used the channel hardening property to obtain approximate closed-form expressions for the BER of a DCP-ACS system. These expressions were then verified to be in close agreement with the empirical performance using Monte Carlo simulations. It was also shown through simulations that the proposed blind

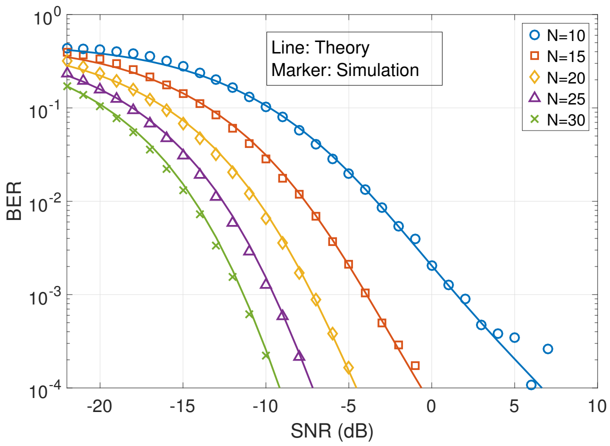

Figure 10. Probability of error in the LSB versus the data SNR for different number of SNs in a 2/4 PAM DCP-ACS system.

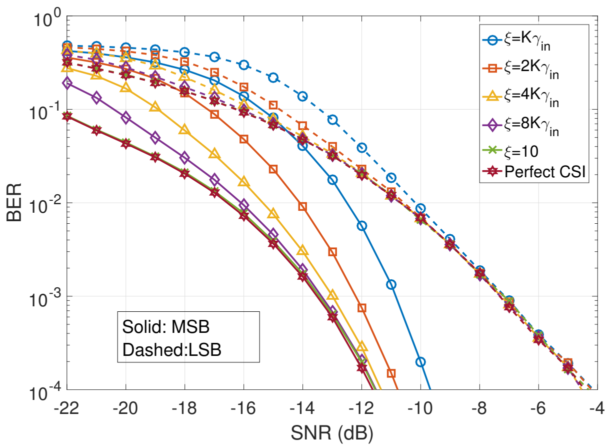

Figure 11. Probability of error in the LSB versus the data SNR for different pilot SNRs (ξ) in a 2/4 PAM DCP-ACS system.

channel estimation algorithm can perform almost as good as the detector with perfect CSI at the FC. Hence, uplink pilots are not necessary. Future work could consider the extension of this work to a system where the SNs transmit different data streams to multiple FCs using ACS [9].

Appendix A
An Alternative Expression for $E[h_m]$

letting $\mathcal{K}_m$ denote the subset of nodes that transmit the mth bit, we can write the channel coefficient h_m as

$$h_m = \sum_{i=1}^{M} g_{mi} \sum_{k=1}^{K} \alpha_k \mathbb{1}_{\{\tau_{i-1} \le \hat{\alpha}_k < \tau_i\}} \mathbb{1}_{\{k \in \mathcal{K}_m\}}. \tag{74}$$

Taking the expectation, we get

$$E[h_m] = \sum_{i=1}^{M} g_{mi} \sum_{k=1}^{K} \Omega_k E[\alpha_k; \tau_{i-1} \le \alpha_k < \tau_i | k \in \mathcal{K}_m] \times \Pr\{k \in \mathcal{K}_m\}. \tag{75}$$

Since $k \in \mathcal{K}_m$ only if $\alpha_k > \tau_{m-1}$,

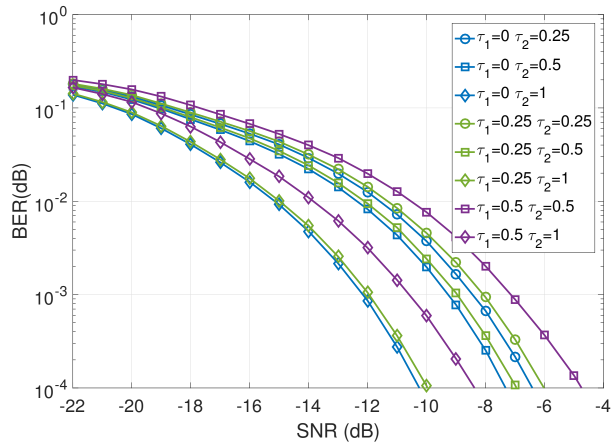

Figure 12. Probability of error in the middle bit versus the data SNR for different values of the thresholds τ_1 and τ_2 in a 2/4/8 QAM DCP-ACS system.

$\Pr\{k \in \mathcal{K}_m\} = f(0; \Omega_k; \tau_{m-1}, \infty)$. Also, defining

$$\bar{f}(p; \Omega; \tau_{i-1}, \tau_i, \tau_{m-1}) \triangleq \frac{f(p; \Omega; \tau_{i-1}, \tau_i)}{f(0; \Omega; \tau_{m-1}, \infty)}, \tag{76}$$

$E[h_m]$ can be written as

$$E[h_m] = \sum_{k=1}^{K} \sqrt{\Omega_k} f(0; \Omega_k; \tau_{m-1}, \infty) \times \sum_{i=1}^{M} g_{mi} \bar{f}(1; \Omega_k; \tau_{i-1}, \tau_i, \tau_{m-1}). \tag{77}$$

Denoting the cardinality of $\mathcal{K}_m$ by κ_m, and considering i.i.d channels, we get

$$E[h_m] = \sum_{k=1}^{K} \sqrt{\Omega} \Pr\{\kappa_m = k\} \sum_{i=1}^{M} k g_{mi} \bar{f}(p; \Omega; \tau_{i-1}, \tau_i, \tau_{m-1}), \tag{78}$$

where $\Pr\{\kappa_m = k\} = \binom{K}{k} f^k(0; \tau_{m-1}, \infty) f^{K-k}(0; 0, \tau_{m-1})$.

References

[1] J. Voas, "Demystifying the internet of things," *Computer*, vol. 49, pp. 80–83, June 2016.

[2] M. A. Razzaque, M. Milojevic-Jevric, A. Palade, and S. Clarke, "Middleware for internet of things: A survey," *IEEE Internet of Things Journal*, vol. 3, pp. 70–95, Feb. 2016.

[3] J. Chamberland and V. Veeravalli, "Wireless sensors in distributed detection applications," *IEEE Signal Process. Mag.*, vol. 24, pp. 16–25, May 2007.

[4] Y.-S. Tu and G. Pottie, "Coherent cooperative transmission from multiple adjacent antennas to a distant stationary antenna through AWGN channels," in *Proc. VTC (Spring)*, pp. 130–134, May 2002.

[5] R. Mudumbai, D. Brown, U. Madhow, and H. Poor, "Distributed transmit beamforming: challenges and recent progress," *IEEE Commun. Mag.*, vol. 47, pp. 102–110, Feb. 2009.

[6] R. Mudumbai, G. Barriac, and U. Madhow, "On the feasibility of distributed beamforming in wireless networks," *IEEE Trans. Wireless Commun.*, vol. 6, pp. 1754–1763, May 2007.

[7] K. Chaythanya, R. Annavajjala, and C. Murthy, "Comparative analysis of pilot-assisted distributed cophasing approaches in wireless sensor networks," *IEEE Trans. Signal Process.*, vol. 59, pp. 3722–3737, Aug. 2011.

[8] R. Mudumbai, J. Hespanha, U. Madhow, and G. Barriac, "Distributed transmit beamforming using feedback control," *IEEE Trans. Inf. Theory*, vol. 56, pp. 411–426, Jan. 2010.

[9] R. Chopra, C. R. Murthy, and R. Annavajjala, "Multistream distributed cophasing," *IEEE Trans. Signal Process.*, vol. 65, pp. 1042–1057, Feb. 2017.

[10] T. Cover, "Broadcast channels," *IEEE Trans. Inf. Theory*, vol. 18, pp. 2–14, Jan. 1972.

[11] K. Ramchandran, A. Ortega, K. M. Uz, and M. Vetterli, "Multiresolution broadcast for digital HDTV using joint source/channel coding," *IEEE J. Sel. Areas Commun.*, vol. 11, pp. 6–23, Jan. 1993.

[12] M. Isaka, M. P. C. Fossorier, R. H. Morelos-Zaragoza, S. Lin, and H. Imai, "Multilevel coded modulation for unequal error protection and multistage decoding. II. asymmetric constellations," *IEEE Trans. Commun.*, vol. 48, pp. 774–786, May 2000.

[13] I.-M. Kim, S. S. Ghassemzadeh, and V. Tarokh, "Optimized nonuniform PSK for multiclass traffic and its application to space-time block codes," *IEEE Trans. Commun.*, vol. 54, pp. 364–373, Feb. 2006.

[14] M. B. Pursley and J. M. Shea, "Nonuniform phase-shift-key modulation for multimedia multicast transmission in mobile wireless networks," *IEEE J. Sel. Areas Commun.*, vol. 17, pp. 774–783, May 1999.

[15] M. B. Pursley and J. M. Shea, "Adaptive nonuniform phase-shift-key modulation for multimedia traffic in wireless networks," *IEEE J. Sel. Areas Commun.*, vol. 18, pp. 1394–1407, Aug. 2000.

[16] L.-L. Yang and L. Hanzo, "A recursive algorithm for the error probability evaluation of M-QAM," *IEEE Commun. Lett.*, vol. 4, pp. 304–306, Oct. 2000.

[17] P. K. Vitthaladevuni and M. S. Alouini, "A recursive algorithm for the exact ber computation of generalized hierarchical QAM constellations," *IEEE Trans. Inf. Theory*, vol. 49, pp. 297–307, Jan. 2003.

[18] S. J. Lee, K. A. Kim, J. S. Jung, and S. C. Lee, "Analytical performance evaluation of hierarchical 16 QAM for multicast/broadcast transmission," *IEEE Commun. Lett.*, vol. 16, pp. 1536–1539, Oct. 2012.

[19] S. H. Chang, M. Rim, P. C. Cosman, and L. B. Milstein, "Optimized unequal error protection using multiplexed hierarchical modulation," *IEEE Trans. Inf. Theory*, vol. 58, pp. 5816–5840, Sept. 2012.

[20] M. M. U. Rahman, R. Mudumbai, and S. Dasgupta, "Consensus based carrier synchronization in a two node networks," in *18th IFAC World Congress*, pp. 10038–10043, June 2011.

[21] S. Zhou and G. Giannakis, "How accurate channel prediction needs to be for transmit-beamforming with adaptive modulation over rayleigh MIMO channels?," *IEEE Trans. Wireless Commun.*, vol. 3, pp. 1285–1294, July 2004.

[22] M. K. Banavar, A. D. Smith, C. Tepedelenlioglu, and A. Spanias, "On the effectiveness of multiple antennas in distributed detection over fading MACs," *IEEE Trans. Wireless Commun.*, vol. 11, pp. 1744–1752, May 2012.

[23] D. Ciuonzo, G. Romano, and P. Salvo-Rossi, "Channel-aware decision fusion in distributed MIMO wireless sensor networks: Decode-and-fuse vs. decode-then-fuse," *IEEE Trans. Wireless Commun.*, vol. 11, pp. 2976–2985, Aug. 2012.

[24] D. Ciuonzo, P. Salvo-Rossi, and S. Dey, "Massive MIMO channel-aware decision fusion," *IEEE Trans. Signal Process.*, vol. 63, pp. 604–619, Feb. 2015.

[25] A. Manesh, C. Murthy, and R. Annavajjala, "Physical layer data fusion via distributed co-phasing with general signal constellations," *IEEE Trans. Signal Process.*, vol. 63, pp. 4660–4672, Sept. 2015.

[26] S. H. Chang, M. Rim, P. C. Cosman, and L. B. Milstein, "Optimized unequal error protection using multiplexed hierarchical modulation," *IEEE Trans. Inf. Theory*, vol. 58, pp. 5816–5840, Sept. 2012.

[27] G. Chrystal, *Algebra, an Elementary Text-book for the Higher Classes of Secondary Schools and for Colleges, Part 2*. Providence, Rhode Island, United States: American Mathematical Society, 1964.

[28] A. Papoulis and S. U. Pillai, *Probability, Random Variables, and Stochastic Processes*. McGraw-Hill Higher Education, 4 ed., 2002.

[29] N. R. Pal and J. C. Bezdek, "On cluster validity for the fuzzy c-means model," *IEEE Trans. Fuzzy Systems*, vol. 3, pp. 370–379, Aug. 1995.

[30] D. T. Anderson, J. C. Bezdek, M. Popescu, and J. M. Keller, "Comparing fuzzy, probabilistic, and possibilistic partitions," *IEEE Trans. Fuzzy Systems*, vol. 18, pp. 906–918, Oct. 2010.

[31] T. C. Havens, J. C. Bezdek, C. Leckie, L. O. Hall, and M. Palaniswami, "Fuzzy c-means algorithms for very large data," *IEEE Transactions on Fuzzy Systems*, vol. 20, pp. 1130–1146, Dec. 2012.

[32] T. Narasimhan and A. Chockalingam, "Channel hardening-exploiting message passing (CHEMP) receiver in large-scale MIMO systems," *IEEE J. Sel. Topics Signal Process.*, vol. 8, pp. 847–860, Oct. 2014.

[33] G. R. Wood, "The bisection method in higher dimensions," *Mathematical Programming*, vol. 55, no. 1, pp. 319–337, 1992.

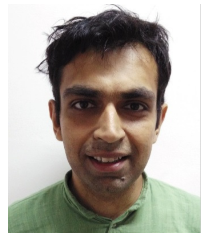

Ribhu Chopra received the B.E. degree in Electronics and Communication Engineering from Panjab University, Chandigarh, India in 2009, and the M. Tech. and Ph. D. Degrees in Electronics and Communication Engineering from the Indian Institute of Technology Roorkee, India in 2011 and 2016 respectively. He worked as a project associate at Department of Electrical Communication Engineering, Indian Institute of Science, Bangalore from Aug. 2015, till May 2016. From May 2016 to March 2017 he worked as an institute research associate at the Department of Electrical Communication Engineering, Indian Institute of Science, Bangalore, India. In April 2017, he joined the department of Electronics and Electrical Engineering, Indian Institute of Technology Guwahati, Assam, India. His research interests include statistical and adaptive signal processing, massive MIMO communications, and cognitive communications.

Ramesh Annavajjala (S'03–M'06–SM'10) is an affiliated research associate professor at the College of Computer and Information Science, Northeastern University, Boston, MA, USA. He is also affiliated with Draper, an independent and non-profit organization, at Cambridge, MA, USA. Earlier, he served as the Distinguished Member of Technical Staff at the Altiostar Networks Inc., a Tewksbury, MA, based start-up company developing cloud-RAN optimized 4G LTE base-station products. Prior to that, he was a Principal Member of Research Staff at the Mitsubishi Electric Research Labs (MERL), in Cambridge, MA. He has also held industry positions at ArrayComm LLC (San Jose, CA, USA), Synopsys Inc., (Bangalore, India) and CMC R&D Center (Hyderabad, India). He received the Bachelors in Electronics and Communication Engineering from the National Institute of Technology (NIT, Warangal, India, May 1998), Masters in Telecommunications from the Indian Institute of Science (IISc, Bangalore, India, Jan. 2001), and Ph.D. in Electrical Engineering from the University of California at San Diego (UCSD, La Jolla, CA, June 2006).

Dr. Annavajjala was a recipient of the Purkayastha/TimeLine Ventures graduate fellowship (2002-2003), a co-recipient of the best paper award from the IEEE WPMC 2009 conference, and was a guest editor for the special issue on **Wireless Cooperative Networks** of the EURASIP Journal on Advanced Signal Processing. He is a Senior Member of the IEEE, and was nominated for the MIT TR-35. He has published more than 60 papers in international journals and conferences, made numerous contributions to commercial wireless standards, and is a co-inventor of 10 US patents (granted).

Chandra R. Murthy (S'03–M'06–SM'11) received the B. Tech. degree in Electrical Engineering from the Indian Institute of Technology Madras, India, in 1998, the M. S. and Ph. D. degrees in Electrical and Computer Engineering from Purdue University and the University of California, San Diego, USA, in 2000 and 2006, respectively. From 2000 to 2002, he worked as an engineer for Qualcomm Inc., where he worked on WCDMA baseband transceiver design and 802.11b baseband receivers. From Aug. 2006 to Aug. 2007, he worked as a staff engineer at Beceem Communications Inc. on advanced receiver architectures for the 802.16e Mobile WiMAX standard. In Sept. 2007, he joined the Department of Electrical Communication Engineering at the Indian Institute of Science, Bangalore, India, where he is currently working as an Associate Professor.

His research interests are in the areas of energy harvesting communications, multiuser MIMO systems, and sparse signal recovery techniques applied to wireless communications. His paper won the best paper award in the Communications Track in the National Conference on Communications 2014. He has 45+ journal papers and about 80 conference papers to his credit. He was an associate editor for the IEEE Signal Processing Letters during 2012-16. He is an elected member of the IEEE SPCOM Technical Committee for the years 2014-16. He is currently serving as the Chair of the IEEE Signal Processing Society, Bangalore Chapter, and as an associate editor for the IEEE Transactions on Signal Processing, Sadhana and as an editor for the IEEE Transactions on Communications.